## Conclusions

A three-dimensional, pressure-based CFD method is used to benchmark an experimental investigation of base flowfield for a four-engine clustered nozzle. The result of the analysis supported Brewer's inviscid flow theory[1] that the lateral flow emanating from behind the detached shock portion of the plume impingement dominated the creation of the reverse jet. It also goes one step further by showing that the strength of the reverse jet is determined by the viscous effect. In addition, computationally efficient base flowfield solution is obtained through Prandtl–Meyer expansion resolved grid treatment.

## References

[1]Brewer, E. B., and Craven, C. E., "Experimental Investigation of Base Flow Field at High Altitude for a Four-Engine Clustered Nozzle Configuration," NASA TND-5164, Feb. 1969.

[2]Wang, T.-S., and Chen, Y.-S., "Unified Navier-Stokes Flowfield and Performance Analysis of Liquid Rocket Engines," *Journal of Propulsion and Power*, Vol. 9, No. 5, 1993, pp. 678–685.

[3]Korst, H. H., Chow, W. L., and Zumwalt, G. W., "Research on Transonic and Supersonic Flow of a Real Fluid at Abrupt Increases in Cross Section," ME Tech. Rept. 392-5, Univ. of Illinois, Urbana, IL, 1959.

# Beam Waist/Focus Misalignment Error Estimates in Laser Doppler Anemometry

Clinton L. Dancey* and Jeffrey Hetmanski†
*Virginia Polytechnic Institute and State University, Blacksburg, Virginia 24061*

## Introduction

If the Gaussian beam waists in a path-compensated, dual-beam, fringe-mode laser Doppler anemometer (LDA) are coincident with the focus of the two beams (the point where the axes of the two beams cross), the interference fringe spacing at the focus $d_{fm}$ is given by the familiar expression:

$$d_{fm} = \lambda/2 \sin(\kappa) \tag{1}$$

where $\lambda$ is the laser wavelength and $\kappa$ is the half-angle between the two transmission beams. If, on the other hand, the beam waists are misaligned, and therefore, not coincident with the focus, the fringe spacing $d_f$ varies with position within the beam crossover region[1–5] and the nonuniformity of $d_f$ within the LDA measurement volume results in mean fringe bias[5] and broadening errors.[1,3] Broadening error has been treated elsewhere, whereas mean fringe bias error, by comparison, has received relatively little attention. In this Note, the nature and magnitude of mean fringe bias error is considered. Specifically, it is shown that the "average" fringe spacing within the LDA measurement volume differs from that given by Eq. (1), even for "aligned" systems, and that the error is relatively insensitive to the degree of misalignment. It is also demonstrated by way of an illustration that the magnitude of the error is small for many practical LDA laser and optical arrangements.

Received Oct. 28, 1993; revision received Aug. 1, 1994; accepted for publication Sept. 20, 1994. 

*Assistant Professor, Department of Mechanical Engineering. Member AIAA.

†Research Assistant, Department of Mechanical Engineering.

## Background

Mean fringe bias error occurs since the computed fringe spacing based upon Eq. (1) and the measured angle $\kappa$ only applies at the focus.[1] To illustrate, if it is assumed that the flow velocity is uniform and steady, the computed mean velocity, obtained from a large ensemble of individual measurements distributed over the measurement volume and utilizing the familiar equation

$$V = \nu d_{fm} \tag{2}$$

(where $\nu$ is the Doppler frequency and $V$ is the velocity component perpendicular to the bisector of the two transmission beams), may be biased away from the true uniform steady value due to the unaccounted for variation of $d_f$ within the measurement volume.

Alternatively, mean fringe bias may be described by defining an average or mean fringe spacing within the LDA measurement volume and comparing it to that given by Eq. (1). This is the approach taken in this Note. (Other forms of bias that may occur in LDA are neglected in this work.)

## Mean Fringe Spacing

In a path-compensated dual-beam LDA $d_f$ may be considered a function of position within the beam crossover region. That is $d_f(\xi)$, where $\xi$ is a position variable. The mean fringe spacing $\langle d_f \rangle$ within the measurement volume is defined here by a conventional average:

$$\langle d_f \rangle = \left[ \int_{\xi_m - L}^{\xi_m + L} d_f(\zeta)\, \mathrm{d}\zeta \right] \Big/ 2L \tag{3}$$

where $\xi_m$ is the focus location and $2L$ is the length of the measurement volume.

In this Note, Hanson's theory of fringe divergence is used to derive an expression for $d_f(\xi)$ and Eq. (3) is employed to obtain $\langle d_f \rangle$. An equation for the fractional mean fringe bias

$$\frac{\langle d_f \rangle - d_{fm}}{d_{fm}} = \frac{\langle d_f \rangle}{d_{fm}} - 1 \tag{4}$$

is derived and the functional dependence of the bias on relevant LDA system parameters is made explicit. Finally, an illustrative example is presented.

## Mean Fringe Bias Error

The front transmission lens and one of the two Gaussian beams of a dual beam LDA are shown in the sketch of Fig. 1. The focal distance $f$ shown in the figure is the location (measured from the lens) where the centerline axes of the two laser beams cross. $z_1$ is the location of the beam waist (again measured from the lens). For the path-compensated case, and with some approximating assumptions, Hanson[1,2] showed that the variation in the Doppler frequency within the beam crossover region (which is not shown in the figure), is given by

$$\frac{\mathrm{d}\nu}{\nu\, \mathrm{d}\xi} = -\frac{1}{\xi[1 + (\pi\omega_1^2/\lambda\xi)^2]} \tag{5}$$

where $\xi$ is the distance measured from the waist (see Fig. 1) along the dual-beam bisector to an arbitrary location within

the crossover region. $\omega_1$ is the radius of the beam waist "downstream" of the lens and $d\nu$ is the shift in the Doppler frequency due to a displacement within the crossover region of $d\xi$. For constant velocity $V$, Eq. (2) yields

$$\frac{d\nu}{\nu\, d\xi} = -\frac{1}{d_f}\frac{d(d_f)}{d\xi} \tag{6}$$

and so Eq. (5) also gives the fractional rate of change of fringe spacing in the crossover region. Integration of Eq. (5) together with Eq. (6) and assuming $\omega_1$ is constant, yields

$$\frac{d_f}{d_{fm}} = \sqrt{\left\{\frac{1 + [\xi^2/(\pi\omega_1^2/\lambda)^2]}{1 + [(z_1 - f)^2/(\pi\omega_1^2/\lambda)^2]}\right\}} \tag{7}$$

for the fringe spacing as a function of position within the crossover region (recalling that $\xi$ is measured from the waist). $d_{fm}$ is the fringe spacing at the center of the crossover region (the focus) and is given by Eq. (1).[1] The magnitude of $z_1 - f$, which has the dimension of length, is termed here the downstream waist/focus misalignment and physically represents the distance between the beam waist and the focus point.

It is apparent from Eq. (7) that even for aligned systems, i.e., $z_1 = f$, the fringe spacing is not constant within a measurement volume of finite length since $d_f$ remains a function of $\xi$ and $\xi$ varies from one end of the volume to the other. It is also clear from Eq. (7) that the fringe spacing variation within the volume depends upon the length of the volume, the size of the misalignment, and the characteristic length, $c = \pi\omega^2/\lambda$.

Integrating in Eq. (3) with Eq. (7) for $d_f(\xi)$ yields

$$\begin{aligned}\frac{\langle d_f\rangle}{d_{fm}} = {} & \frac{1}{4\dfrac{L}{c}\sqrt{1 + \left[\dfrac{(z_1 - f)}{c}\right]^2}} \\ & \times \left[\frac{(z_1 - f)}{c} + \frac{L}{c}\right]\sqrt{1 + \left[\frac{(z_1 - f)}{c} + \frac{L}{c}\right]^2} \\ & - \left[\frac{(z_1 - f)}{c} - \frac{L}{c}\right]\sqrt{1 + \left[\frac{(z_1 - f)}{c} - \frac{L}{c}\right]^2} \\ & + \ln\left\{\frac{\left[\dfrac{(z_1 - f)}{c} + \dfrac{L}{c}\right] + \sqrt{\left[\dfrac{(z_1 - f)}{c} + \dfrac{L}{c}\right]^2 + 1}}{\left[\dfrac{(z_1 - f)}{c} - \dfrac{L}{c}\right] + \sqrt{\left[\dfrac{(z_1 - f)}{c} - \dfrac{L}{c}\right]^2 + 1}}\right\}\end{aligned} \tag{8}$$

where $2L$ is the length of the measurement volume and in Eq. (3) $\xi_m = (z_1 - f)$ is the focus point. Equation (8) can be used to compute the mean fringe bias error once $L$, $c$, and the downstream misalignment are specified. However, expanding the right-hand side (RHS) of Eq. (8) for small $L/c$ is not unreasonable for many practical LDA designs. The result when substituted into Eq. (4) for the fractional mean fringe bias is

$$(\langle d_f\rangle/d_{fm}) - 1 = \mathcal{O}[(L/c)^2] \tag{9}$$

Equation (9) is the principle result of this Note. From this equation it may be concluded that, to order $(L/c)^2$, mean fringe bias error is independent of the downstream misalignment and if the effective length of the measurement volume is small compared to the characteristic length $c$, to an excellent approximation, the average fringe spacing about the focus is equal to the local fringe spacing at the focus [given by Eq. (1)].

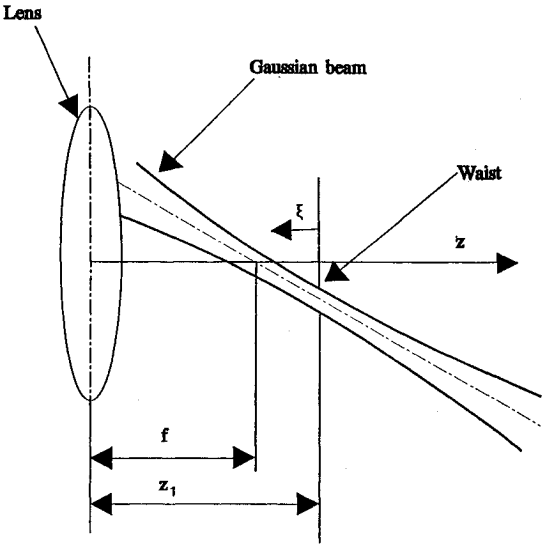


**Fig. 1 Sketch of focused Gaussian beam with waist misaligned.**

## Example

For illustrative purposes the LDA experimentally investigated by Hanson (to verify his theory of fringe divergence and broadening error) is reanalyzed here for mean fringe bias error.

Hanson employed an argon ion laser with $\lambda = 514.5$ nm and a dual beam spacing of 10 cm in his experiments. The upstream waist radius and upstream waist position (measured relative to the lens) were 0.06 and 200 cm, respectively. Two different focal lengths were investigated.

1) For $f = 43.5$ cm the downstream waist/focus misalignment was 11.5 cm and the measurement volume length was determined to be approximately 0.5 cm. The fringe broadening error is estimated at approximately 4.3% using Hanson's theory and compares favorably with the measured broadening. Using the theory presented previously for mean fringe bias error, one obtains $c = 2.58$ cm and a mean fringe bias error [from Eq. (9)] of order 1%.

2) For $f = 29.5$ cm the downstream misalignment was 2.5 cm and the length of the measurement volume was estimated as 0.1 cm. In this case Hansen's theory predicts a fringe broadening error of 2% and the present analysis gives a mean fringe bias error of order 0.04%. In either case, although the broadening error may be significant, the mean fringe bias error is of the same order or smaller than other sources of uncertainty typically associated with fringe mode LDA measurements.[6]

Similar calculations are possible for adequately specified commercial LDA systems. For many such systems it is easily verified with Eq. (8) and the equations for Gaussian beam propagation that the mean fringe bias error is small and only very weakly dependent upon the waist/focus misalignment.

It is emphasized, however, that the previous analysis assumes the average in Eq. (3) is taken about the transmission focus, where Eq. (1) is applicable. The mean fringe bias error is generally small in this case because the contributions from each side of the focus tend to cancel each other. If the fringes were straight and divergent, the two contributions would cancel completely and a zero mean bias would result. Because the fringes have curvature, a small nonzero bias is present. If, on the other hand, the LDA-receiving optics are focused away from the center of the crossover region (as may occur with off-axis collection), a larger, perhaps significant mean fringe bias error is possible, since the averaging of Eq. (3) now occurs about a point other than the focus of the trans-

mission lens. The magnitude of the bias error in this case is bounded, however, by the broadening error limit of Hanson. In this event, if the mean bias error is judged excessive, it could be removed by use of a calibration flow, to, in effect, determine the average fringe spacing at the receiving optics focus.

## References

[1]Hanson, S., "Broadening of the Measured Frequency Spectrum in a Differential Laser Anemometer Due to Interference Plane Gradients," *Journal of Physics D: Applied Physics*, Vol. 6, No. 2, 1973, pp. 164–171.

[2]Hanson, S., "Visualization of Alignment Errors and Heterodyning Constraints in Laser Doppler Velocimeters," *Proceedings of the LDA Symposium* (Copenhagen), 1975, pp. 176–182.

[3]Durst, F., and Stevenson, W. H., "Moiré Patterns to Visually Model Laser-Doppler Signals," *Proceedings of the LDA Symposium* (Copenhagen), Hemisphere, Washington, DC, 1975, pp. 183–202.

[4]Durst, F., and Stevenson, W. H., "Properties of Focused Laser Beams and the Influence on Optical Anemometer Signals," *Proceedings of the Minnesota Symposium on Laser Anemometry*, Univ. of Minnesota, Dept. of Conferences, Minneapolis, MN, 1975, pp. 371–388.

[5]Young, W. H., Meyers, J. F., and Hepner, T. E., "Laser Velocimeter Systems Analysis Applied to a Flow Survey Above a Stalled Wing," NASA TN D8408, 1977.

[6]Rabe, D. C., and Dancey, C. L., "Comparison of Laser Transit and Laser Doppler Anemometer Measurements in Fundamental Flows," AIAA Paper 86-1650, June 1986.

# New Supersonic Combustion Research Facility

M. R. Gruber* and A. S. Nejad†
*U.S. Air Force Wright Laboratory, Wright–Patterson Air Force Base, Ohio 45433*

## Introduction

A NEW research facility designed to allow studies of the basic mechanisms governing the mixing and combustion processes within realistic supersonic combustor geometries has been developed. With the push toward hypersonic flight regimes, such a facility provides a clear forum for enhancing the basic knowledge and databases through the use of conventional and advanced diagnostic techniques. The facility is capable of variable Mach number, continuous flow operation with a wide variety of conditions. Emphasis was placed on optical access to the nominally 5 × 6 in. test section; the resulting design utilizes four windows to allow visualization of all three orthogonal flow planes. Pitot rake studies reveal a uniform, two-dimensional, Mach 1.98 stream at the entrance to the test section. A slight decrease (2%) in freestream Mach number in the streamwise direction exists within the test section; however, the flow appears symmetric about the transverse and spanwise centerlines. Boundary-layer development is also documented.

Received Oct. 22, 1993; presented as Paper 94-0544 at the AIAA 32nd Aerospace Sciences Meeting and Exhibit, Reno, NV, Jan. 10–13, 1994; revision received Oct. 31, 1994; accepted for publication Dec. 5, 1994. This paper is declared a work of the U.S. Government and is not subject to copyright protection in the United States.

*Aerospace Engineer, Advanced Propulsion Division, Experimental Research Branch. Member AIAA.

†Senior Research Engineer, Advanced Propulsion Division, Experimental Research Branch. Member AIAA.

## Facility Design

The underlying objective of this design effort was to develop an in-house research facility capable of allowing studies of the enhancement and control of fuel-air mixing in supersonic combustors with conventional and state-of-the-art, nonintrusive diagnostic techniques. Other design objectives of considerable importance were: variable Mach number, continuous flow operation, peak stagnation conditions of 400 psig and 1660°R at a peak flow rate of 34 lbm/s, nominal 5 × 6 in. test section with allowances for nozzle boundary-layer growth, high degree of optical access to the test section, modularity for ease of maintenance and future facility enhancement, and thermal expansion compensation to minimize test section movement. Figure 1a is a schematic of the result of the design effort, the design features are described in the following text.

### Air Supply System

A series of compressors and a gas-fired heat exchanger are available to produce high-pressure/high-temperature air for use in the new laboratory. A hot line capable of supplying 17 lbm/s of 750-psig air at 1660°R and a cold line capable of supplying 17 lbm/s of 750-psig air at ambient temperature are used in tandem to produce the desired stagnation conditions. The two supply lines merge at a mixing station, and an insulated expansion loop transports the resulting mixed air to a supply manifold with five branches. Three branches supply air to the clean room, while the other two branches exit out through the roof (a vent line and a pressure relief line).

### Flow Facility

Five major components comprise the combustion tunnel: 1) the inlet section, 2) settling chamber, 3) nozzle section, 4) test section, and 5) the diffuser (see Fig. 1a). All were designed in accordance with the ASME piping code.[1] The inlet section transports air from the supply manifold described above to the settling chamber. Six flexible stainless steel hoses connect the upper and lower manifolds and allow for thermal growth in the upstream direction. The lower manifold, block valve, and expansion section mount onto support carts that roll on a pair of rails. These carts allow for maintenance and additional thermal growth management. A rearward-facing perforated cone is housed within the expansion section to distribute the flow as it enters the 24-in. settling chamber.

The settling chamber uses an array of mesh screens and a section of honeycomb to condition the flow prior to acceleration by the supersonic nozzle. This chamber is designed to withstand 400 psig at 1660°R, while its size produces air velocities of approximately 50 ft/s over the range of desired tunnel operating conditions. Pressure and temperature sensors are installed to provide documentation and feedback to the control system. Finally, a transition region required by the change in geometry from the axisymmetric settling chamber to the planar nozzle section is housed at the downstream end of this chamber. The entire section mounts to a support stand that carries its weight and the force due to the subatmospheric pressure of the exhauster system.

Planar two-dimensional nozzles have been designed ($M$ = 2, 3, 4.5) using a method of characteristics code developed by Carroll et al.[2] This code computes the contour of a continuous slope converging–diverging nozzle yielding a uniform exit flow aligned with the nozzle axis. Boundary-layer growth is not accounted for in this inviscid code. However, correction for viscous effects is accomplished using boundary-layer displacement thickness calculations resulting from Burke's equation,[3] which relates the local turbulent boundary-layer dis-